Adaptive remodeling of skeletal muscle energy metabolism in high-altitude hypoxia: Lessons from AltitudeOmics

Received for publication, October 16, 2017, and in revised form, March 1, 2018 Published, Papers in Press, March 14, 2018, DOI 10.1074/jbc.RA117.000470

Adam J. Chicco[‡§1], Catherine H. Le[§], Erich Gnaiger[¶], Hans C. Dreyer[‖], Jonathan B. Muyskens[‖], Angelo D'Alessandro[**], Travis Nemkov[**], Austin D. Hocker[‖], Jessica E. Prenni[‡‡], Lisa M. Wolfe[‡‡], Nathan M. Sindt[‡‡], Andrew T. Lovering[‖], Andrew W. Subudhi[§§], and Robert C. Roach[¶¶]

From the Departments of [‡]Biomedical Sciences, [§]Cell and Molecular Biology, and [‡‡]Biochemistry and Molecular Biology, Colorado State University, Fort Collins, Colorado 80523, the [§§]Department of Biology, University of Colorado, Colorado Springs, Colorado 80918, the [¶]Medical University of Innsbruck, 6020 Innsbruck, Austria, the [‖]Department of Human Physiology, University of Oregon, Eugene, Oregon 97403-1240, and the [**]Department of Biochemistry and Molecular Genetics and [¶¶]Altitude Research Center, University of Colorado-Anschutz Medical Campus, Aurora 80045, Colorado 80045

Edited by Jeffrey E. Pessin

Metabolic responses to hypoxia play important roles in cell survival strategies and disease pathogenesis in humans. However, the homeostatic adjustments that balance changes in energy supply and demand to maintain organismal function under chronic low oxygen conditions remain incompletely understood, making it difficult to distinguish adaptive from maladaptive responses in hypoxia-related pathologies. We integrated metabolomic and proteomic profiling with mitochondrial respirometry and blood gas analyses to comprehensively define the physiological responses of skeletal muscle energy metabolism to 16 days of high-altitude hypoxia (5260 m) in healthy volunteers from the AltitudeOmics project. In contrast to the view that hypoxia down-regulates aerobic metabolism, results show that mitochondria play a central role in muscle hypoxia adaptation by supporting higher resting phosphorylation potential and enhancing the efficiency of long-chain acylcarnitine oxidation. This directs increases in muscle glucose toward pentose phosphate and one-carbon metabolism pathways that support cytosolic redox balance and help mitigate the effects of increased protein and purine nucleotide catabolism in hypoxia. Muscle accumulation of free amino acids favor these adjustments by coordinating cytosolic and mitochondrial pathways to rid the cell of excess nitrogen, but might ultimately limit muscle oxidative capacity *in vivo*. Collectively, these studies illustrate how an integration of aerobic and anaerobic metabolism is required for physiological hypoxia adaptation in skeletal muscle, and highlight protein catabolism and allosteric regulation as unexpected orchestrators of metabolic remodeling in this context. These findings have important implications for the management of hypoxia-related diseases and other conditions associated with chronic catabolic stress.

Metabolic adaptations to hypoxia underlie phenotypic responses to a diverse range of physiologic and pathogenic stimuli. Responses of skeletal muscle metabolism to reduced oxygen availability are thought to influence physical capacity and systemic energy homeostasis in high-altitude environments (1), heart failure (2), and chronic obstructive pulmonary disease (3, 4). However, the metabolic adjustments that facilitate physiological adaptation to hypoxia remain unclear, and must be defined to distinguish adaptive from maladaptive changes in hypoxia-related conditions. Despite longstanding interest in this topic (5, 6), consensus on fundamental aspects of muscle metabolism in hypoxia remains elusive, particularly regarding mitochondria (7, 8), the primary site of organismal energy metabolism and oxygen utilization.

Early reports of higher oxidative enzyme activities in muscle from humans and animals residing at high altitude led to the hypothesis that an enhanced capacity for aerobic metabolism is essential for survival in hypoxic environments (9). This idea was later challenged by evidence for lower mitochondrial volume density in high-altitude natives (10) and lowlanders following mountaineering expeditions (11, 12). However, despite these decrements, both populations exhibit preserved or enhanced muscle energetics and work capacity in hypoxia following prolonged exposure (13, 14), suggesting that improvements in bioenergetic efficiency may be the signature of successful hypoxia adaptation (5).

The discovery and characterization of hypoxia-inducible factor-1α (HIF-1α)[2] provided a mechanism for coordinated tran-

This work was supported in part by U.S. Department of Defense Grants W81XWH-11-2-0040 TATRC (to R. C. R.), W81XWH-10- 2-0114 (to A. T. L.), National Institutes of Health NICHID Grant K01HD057332 (to H. C. D.), Grant T32 HL007171 from the National Institutes of Health, NHLBI (to T. N.), Oroboros Instruments, Innsbruck, Austria, the Mitochondrial Physiology Laboratory at Colorado State University, the Altitude Research Center, and the Charles S. Houston Endowed Professorship, Department of Medicine, University of Colorado, Denver. E. G. is Chief Executive Officer of Oroboros Instruments, Innsbruck, Austria. The content is solely the responsibility of the authors and does not necessarily represent the official views of the National Institutes of Health.

This article contains "Materials and methods," Tables S1 and S2, and Figs. S1–S3.

[1] To whom correspondence should be addressed. E-mail: adam.chicco@colostate.edu.

[2] The abbreviations used are: HIF-1α, hypoxia inducible factor-1α; SL, sea level; ETS, electron transfer system; RER, respiratory exchange ratio; OXPHOS, oxidative phosphorylation; CI, Complex I; PCr, phosphocreatine; CK, creatine kinase; Cr, creatine; PNC, purine nucleotide cycle; MAS, malate–aspartate shuttle; PFK, phosphofructokinase; PPP, pentose phosphate pathway; GAPDH, glyceraldehyde-3-phosphate dehydrogenase; PK, pyruvate kinase; PGK, phosphoglycerate kinase; α-KG, α-ketoglutarate; BCAA, branched-chain amino acid; CAC, citric acid cycle; ME1, malic enzyme; HB, hydroxybutyrate; CPT, carnitine palmitoyltransferase; VLCAD, very-long-chain acyl-CoA dehydrogenase; TFP, trifunctional protein complex; AMPK, AMP-activated protein kinase; OPA1, optic atrophy 1; PPARα, proliferator-activated receptor α; FDR, false discovery rate.

scriptional reprogramming of cellular metabolism in hypoxia, which generally favors glycolytic over mitochondrial metabolism (15, 16) and improved oxygen binding by cytochrome oxidase (17). This pattern is consistent with some (12, 18), but not all studies of muscle metabolism at high altitude (19–22). This likely reflects the complex interplay of factors known to influence metabolic substrate supply and demand in hypoxic environments (7), and emphasizes that changes in selected "marker" enzymes or transcriptional regulators might not fully represent adaptive metabolic responses. More recent application of "omics" approaches and high-resolution mitochondrial respirometry have begun to shed light on the complexity of muscle metabolic adjustments to hypoxia (23–25). However, the integrated responses that balance energy demands and stress signals to maintain muscle homeostasis remain unclear, particularly in the absence of additional energetic stress that often accompanies studies of human hypoxia adaptation (*i.e.* trekking or climbing) (12, 25).

In the present study, we combined targeted metabolomic and proteomic profiling of skeletal muscle with mitochondrial respirometry and systemic metabolic assessments of healthy volunteers from the AltitudeOmics expedition (26) at their resident altitude near sea level and following 16 days of high-altitude hypoxia acclimatization. We hypothesized that integrating these complimentary approaches would elucidate previously undiscovered physiological shifts in muscle substrate utilization that resolve some of the longstanding controversies in the field (7). Our results reveal a cooperative rearrangement of cytosolic and mitochondrial metabolism that argues against a classic shift from aerobic to anaerobic energy supply as the primary aim of physiological hypoxia adaptation in skeletal muscle. Rather, we identify protein and purine nucleotide catabolism as major orchestrators of metabolic remodeling through allosteric and substrate-level regulatory mechanisms, which redirect glucose utilization and favor more efficient fatty acid oxidation in combination with subtle stoichiometric shifts in metabolic enzyme expression. This integrative view of muscle metabolism at high altitude provides a new foundation for understanding physiological responses to hypoxia and catabolic stress.

Results and discussion

Systemic responses to high-altitude hypoxia

Study participants (7 male, 7 female; 21 ± 2 years of age) were a subset of 21 individuals involved in the AltitudeOmics project (26). All were healthy Caucasians born and raised below 1500 m, and had not traveled to altitudes >1000 m for at least 3 months before the study. Selected physiological parameters were collected at their resident altitude near sea level (SL; Eugene, OR, 131 m), immediately upon reaching the laboratory at 5260 m ~1 month later (A1; Mt. Chacaltaya, Bolivia), and following 16 days of habitual daily activity at the same altitude (A16) (Table 1). Participants were transported to the high-altitude camp by automobile to standardize the hypoxic exposure and avoid the energetic demands of trekking during acclimatization. Body weight loss occurred from A1 to A16 as expected (27), but was limited by encouraging habitual intake of carbohydrate, fat, and protein dietary sources and light daily activity to minimize effects of negative energy balance, exertional stress, and inactivity. All participants exhibited reductions in resting blood oxygen transport (oxyhemoglobin saturation and arterial PO_2) at A1 that partially recovered at A16, consistent with the classic hypoxia acclimatization response (28). Maximal oxygen uptake (VO_2max) was typical of healthy, recreationally active individuals at SL, and was depressed at A1 and A16, reflecting well-established limitations of hypoxia on the maximal rate of tissue oxygen utilization. The resting respiratory exchange ratio (RER; VCO_2/VO_2) also declined and remained lower throughout hypoxia, indicating a persistent shift in resting metabolic substrate utilization.

Table 1
Physiological responses to high-altitude hypoxia

Data were collected at sea level (SL; Eugene, OR, 131 m), immediately upon reaching the laboratory at 5260 m (A1; Mt. Chacaltaya, Bolivia), and following 16 days of exposure to the same altitude (A16). Data are mean ± S.E. of data obtained only from the 14 subjects used in the present study, reported previously as part of the larger AltitudeOmics cohort (26). The following abbreviations are used: SaO_2, arterial oxyhemoglobin saturation; PaO_2, arterial partial pressure of oxygen; VO_2max , maximal oxygen consumption during a stationary cycling time trial; RER, respiratory exchange ratio (ratio of expired CO_2 to O_2 uptake under resting conditions).

	SL	A1	A16
Body weight (kg)	70 ± 3	71 ± 2	68 ± 2[a]
SaO_2 (%)	98 ± 2	74 ± 1[a]	81 ± 1[a,b]
PaO_2 (mm Hg)	102 ± 2	35 ± 1[a]	45 ± 1[a,b]
VO_2max (ml/kg/min)	49 ± 1	32 ± 1[a]	36 ± 2[a]
RER (VCO_2/VO_2)	0.96 ± 0.03	0.84 ± 0.02[a]	0.82 ± 0.02[a]

[a] $p < 0.05$ *versus* sea level.
[b] $p < 0.05$ *versus* A1.

Hypoxia improves muscle mitochondrial energetics and increases metabolic substrate availability

A loss of muscle oxidative capacity is a hallmark feature of hypoxia-related disorders, and has been attributed to a decline in tissue mitochondrial content and function (2, 4). Muscle mitochondrial responses to physiological hypoxia are less clear (7), with functional measures often being inconsistent with enzymatic and histological estimates of tissue organelle content (22). To comprehensively investigate muscle mitochondrial energetics, we performed high-resolution respirometry on permeabilized fiber bundles from vastus lateralis muscle biopsies freshly obtained under resting post-absorptive conditions at SL and A16. Two respirometry protocols including up to five metabolic substrates were employed to generate mass-corrected oxygen flux values representing 16 distinct respiratory states as described in Table S1 (complete data in Fig. S1). The maximal (noncoupled) mitochondrial electron transfer system (ETS) capacity of muscle fibers fueled by a combination of carbohydrate (pyruvate), amino acid (glutamate), and fatty acid (palmitoylcarnitine) oxidation was unchanged from SL to A16 (ETS capacity; Fig. 1*A*). However, the ETS capacity of human skeletal muscle exceeds the ADP-stimulated "coupled" oxidative phosphorylation (OXPHOS)-linked respiratory capacity (29), which tended to increase from SL at A16 under identical substrate conditions (Fig. 1*B*). This equated to a 38% increase in OXPHOS coupling control at A16 (Fig. 1*C*), indicating that a greater proportion of mitochondrial respiratory capacity is utilized during ATP synthesis when fueled by convergent substrate oxidation pathways. Collectively, these studies

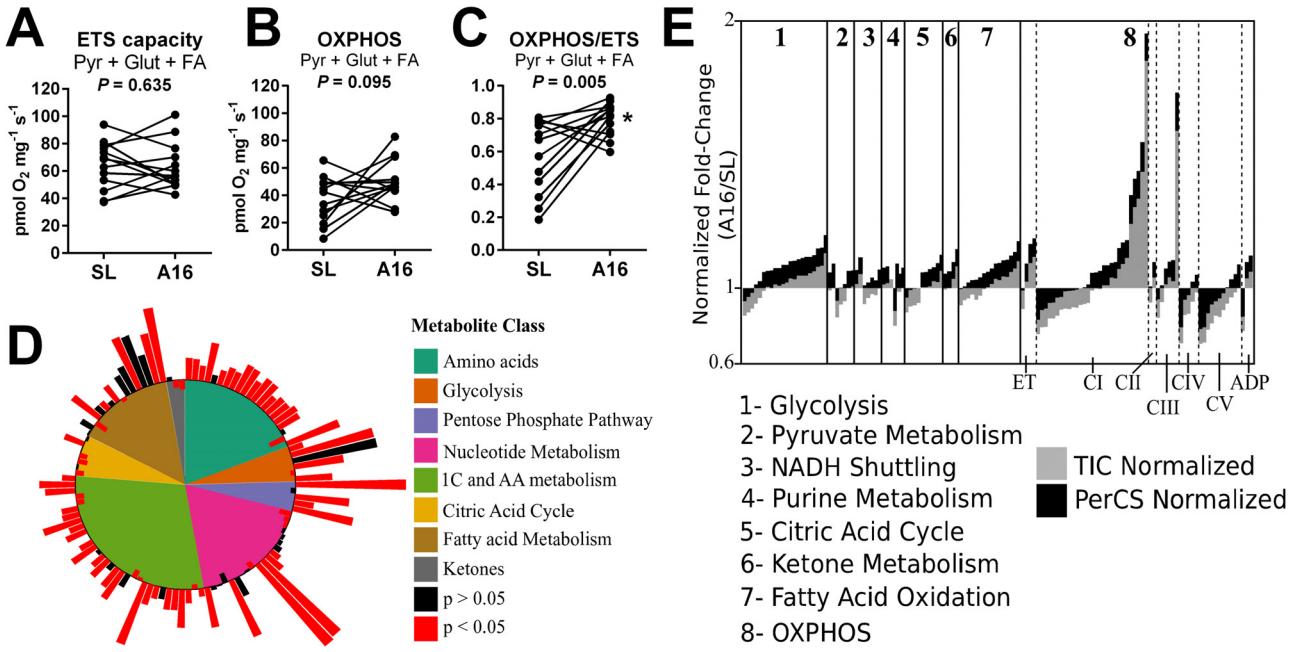

Figure 1. Remodeling of muscle metabolism in hypoxia. *A–C*, mitochondrial respiration in permeabilized muscle fibers fueled by a combination of malate, pyruvate (Pyr), glutamate (Glut), and palmitoylcarnitine (FA) representing the maximal noncoupled ETS capacity (*A*), the maximal ADP-stimulated (OXPHOS) rate (*B*), and OXPHOS coupling control (OXPHOS/ETS; *C*). *D*, summary of targeted LC/MS metabolomic analysis of muscle biopsies (A16/SL; $\log_2$ scale). *E*, summary of tandem-mass tag LC/MS/MS proteomic profiling of muscle biopsies and normalized to total sample peptide ion count (*TIC*, *gray*) or citrate synthase expression (*PerCS*, *black*) corresponding to the data in Table S2b (A16/SL; $\log_2$ scale) (n = 15/group). *CI-V*, complexes I-V of the oxidative phosphorylation (OXPHOS) system; PerCS, normalized to sample citrate synthase; *TIC*, total ion count; *, $p < 0.05$ A16 *versus* SL.

indicate that the mitochondrial respiratory capacity of skeletal muscle is preserved following 16 days of physiological hypoxia, and the existing OXPHOS machinery is more responsive to energy demand (ADP) when abundant mixed substrates are available.

Improved mitochondrial coupling control of muscle fibers at A16 is consistent with the conclusions of previous studies of humans acclimatized to high altitude (23, 25), suggesting an enhancement of muscle bioenergetics in physiological hypoxia. However, results of *in vitro* experiments do not necessarily reflect metabolic substrate handling *in vivo*. Therefore, we performed nontargeted LC/MS metabolomic analyses of flash-frozen sections of the same muscle biopsies at SL and A16, which revealed significant changes in 119 of 250 identified metabolites ($q < 0.05$). These included increases in glycolytic intermediates, amino acids, and fatty acids (Fig. 1*D*), indicating a greater availability of metabolic substrates in hypoxic skeletal muscle under resting conditions *in vivo*. Although this generally reflects greater muscle metabolic flux in hypoxia, variations within major metabolite classes and pathways suggested shifts in substrate utilization that justified more detailed analysis.

Remodeling of the muscle metabolic proteome in hypoxia

To further integrate the findings of respirometry and metabolomic analyses, we next evaluated the expression of 134 intermediary metabolism enzymes identified by tandem-mass tag LC/MS/MS proteomic profiling of the same muscle biopsies at SL and A16 (Fig. 1*E*). Observed changes were generally minor (<20%) with high variability of signals normalized to total ion (peptide) count. Thirty-eight proteins changed significantly from SL to A16 ($q < 0.05$), 31 of which decreased, representing primarily mitochondrial, but also glycolytic pathway enzymes (Table S2). The total ion count of all (120) mitochondrial proteins evaluated (per mg of muscle protein) was unchanged at A16 (97 ± 3% of SL; p = NS). Interestingly, the seven proteins that significantly increased at A16 included key enzymes in glycolysis and fatty acid oxidation, and catalytic subunits of mitochondrial respiratory Complex I (CI). Therefore, hypoxia appears to retain selected components of both cytosolic and mitochondrial muscle metabolism under resting physiological conditions, rather than inducing a global shift from aerobic to anaerobic energy pathways seen in hypoxia-related pathologies (30, 31) and some studies of high-altitude trekkers and climbers (7, 25).

A general reduction in muscle metabolic enzyme content at high-altitude is consistent with previous reports (5, 24), and may reflect a reduction in energy expenditure to improve metabolic efficiency in hypoxia. However, analysis of global (per sample peptide) trends in enzyme expression might not capture relative changes within and between metabolic pathways that mediate important changes in substrate handling, particularly in heterogeneous skeletal muscle samples. We hypothesized that re-evaluating the metabolic proteome relative to a central metabolic "hub" would increase statistical power and facilitate more congruent integration of our datasets. Citrate synthase (CS) was selected as this hub based on its position at the convergence of carbohydrate, protein, and fatty acid catabolism, and its routine use as a marker of muscle oxidative capacity and mitochondrial density (32). Moreover, muscle CS decreased 5% from SL to A16 (Table S2; q = 0.04) despite maintenance of mitochondrial respiratory capacity and improved OXPHOS

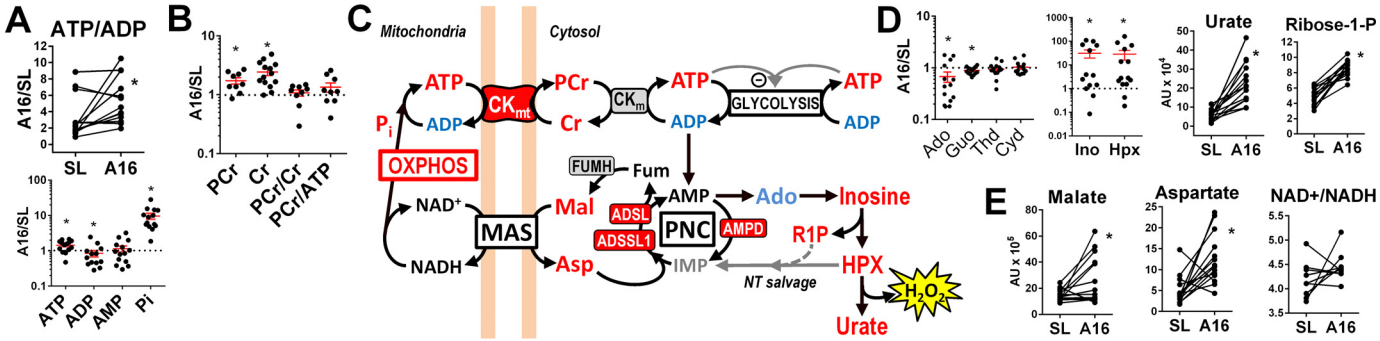

Figure 2. High-energy phosphate and purine nucleotide metabolism. *A* and *B*, muscle adenine nucleotides (*A*) and phosphagen (*B*) changes from SL to A16 detected by LC/MS. *C*, schematic summary of muscle high-energy phosphate and purine nucleotide metabolism. Enzymes that increased relative to CS from SL to A16 ($q < 0.05$) are in *red filled boxes*. Enzymes shown in boxes were found to increase (*red fill*), decrease (*blue fill*), or not change (*gray fill*) from SL to A16 relative to CS in the muscle proteome corresponding to data in Table S2b ($q < 0.05$). Metabolites depicted were found to increase (*red font*), decrease (*blue font*), or not change (*black font*) from SL to A16 ($q < 0.05$), or were undetected (*gray font*) by LC/MS. *D*, changes in muscle nucleosides and purine degradation products from SL to A16. *E*, evidence of elevated MAS activity and stable NADH (NAD) redox status from SL to A16 ($n = 10–14$). *HPX*, hypoxanthine; PNC, purine nucleotide cycle; *, $q < 0.05$ *versus* SL in FDR-adjusted paired *t* tests.

control, suggesting that stoichiometric shifts within the mitochondrial proteome might better explain adaptations of mitochondrial metabolism to hypoxia. As predicted, normalizing enzyme levels to sample CS reduced overall inter-participant signal variability by two-thirds and revealed significant changes in 48 enzymes involved in cytosolic and mitochondrial metabolism, the majority of which increased from SL to A16 (Fig. 1*E*, *black bars*). To elucidate the potential impact of these changes in the metabolic adaptation to hypoxia, we next integrated congruent datasets from proteomic, metabolomics, and respirometry studies in the context of major intermediary metabolic pathways for interpretive analysis, beginning with muscle high-energy phosphate and nucleotide metabolism.

Hypoxia increases resting phosphorylation potential and purine nucleotide turnover

Consistent with an observed improvement of muscle OXPHOS coupling control *in vitro* (Fig. 1*A*), resting muscle ATP levels and the ATP/ADP ratio were higher at A16 compared with SL (Fig. 2*A*). This was accompanied by higher orthophosphate (P_i) and lower ADP content, corroborating *in vivo* evidence from ^{31}P-magnetic resonance spectroscopy on resting gastrocnemius muscles of climbers and trekkers following an expedition to Mount Everest (13). In addition to ADP control of OXPHOS, phosphocreatine (PCr) plays a key role in maintaining cellular ATP levels through the creatine kinase (CK) reaction (33). Muscle PCr and creatine (Cr) increased from SL to A16 to a similar degree as ATP, resulting in stable resting PCr/Cr and ATP/PCr ratios (Fig. 2*B*). Notably, similar increases in resting muscle PCr and ATP were recently reported in high-altitude Sherpas, but not Western lowlanders, following a 2–3 week trekking ascent to Everest Basecamp (5300 m) from Kathmandu (1300 m) (25). This discrepancy in Westerner responses might reflect the confounding energetic stress of mountain trekking during hypoxia acclimatization in untrained lowlanders that was not experienced by our participants, and is plausibly less evident in professional high-altitude porters. Muscle CK isozymes were not uniformly altered by hypoxia in our participants, but expression of the mitochondrial isoform (mtCK) significantly increased relative to CS at A16 (Fig. 2*C*). This could support higher cytosolic ATP levels by maintaining favorable mitochondrial ADP levels to preserve basal OXPHOS levels in hypoxia. Consistent with this interpretation, muscle oxygen extraction is maintained at SL levels at 5260 m (34), suggesting that mitochondria remain the primary source of muscle ATP production under resting conditions. Taken together, these data indicate that acclimatization to physiological hypoxia improves resting muscle phosphorylation potential, perhaps through improved ADP-control of OXPHOS and enhanced phosphagen buffering of mitochondria-derived ATP. In contrast, resting skeletal muscle ATP/ADP and PCr/Cr both decline in chronic obstructive pulmonary disease patients (35), highlighting distinct bioenergetic responses to physiologic *versus* pathologic (or prolonged) hypoxia.

Although the overall adenine nucleotide content of muscle was unchanged from SL to A16, adenosine levels markedly declined, likely due to catabolism evidenced by accumulation of degradation products (Fig. 2*D*). Higher muscle hypoxanthine and urate levels specifically corroborate evidence that purine degradation may be an important source of reactive oxygen species in hypoxic muscle through xanthine oxidase (36). However, muscle AMP levels were maintained at A16, indicating a concomitant activation of nucleotide salvage pathways in conjunction with increased purine nucleotide cycle (PNC) activity. Elevated PNC activity is thought to limit excess energy consumption and acidification of skeletal myocytes in hypoxia by maintaining a high ATP/ADP ratio (37, 38), which favors an allosteric inhibition of glycolytic flux (Fig. 2*C*). All three PNC enzymes significantly increased relative to CS at A16 (Fig. 2*C*; $q < 0.05$), suggesting that this pathway may indeed be favored over conventional oxidative metabolism in hypoxia. Accordingly, the first and rate-limiting enzyme of the PNC, AMP deaminase, is up-regulated by HIF-1α (39). Expression of the subsequent PNC reamination enzymes is regulated by c-Myc (40), which complements HIF-1α to fine-tune metabolic reprogramming of hypoxic cancer cells (41). PNC flux may also be driven by an accumulation of aspartate, which promotes malate–aspartate shuttle (MAS) activity through cytosolic generation of malate from fumarate (Fig. 2*C*). This coupling of the PNC and MAS links purine nucleotide turnover with mito-

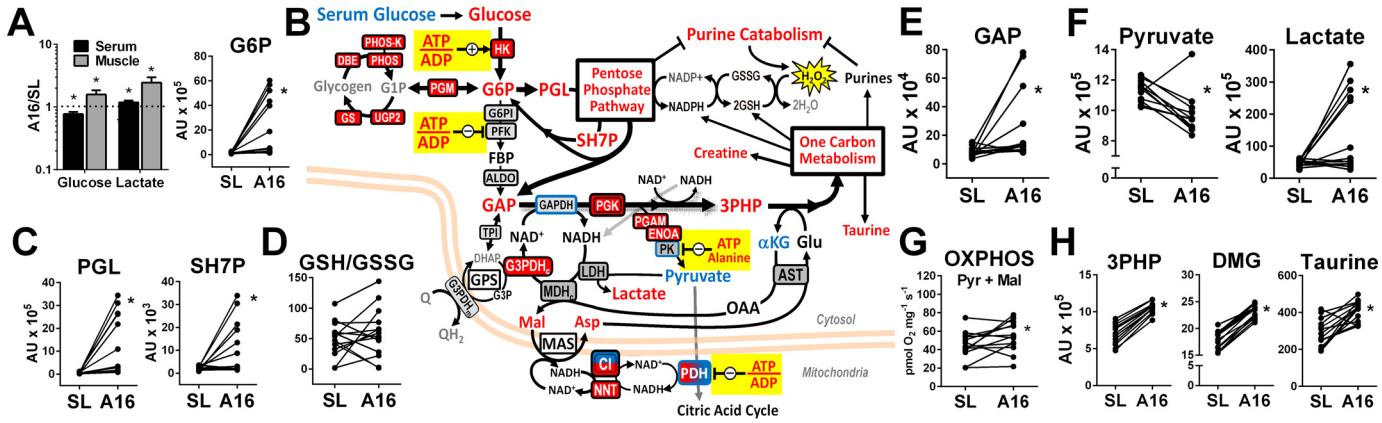

Figure 3. Hypoxia directs muscle glucose toward biosynthetic pathways. *A,* serum and muscle glucose and lactate, and muscle glucose 6-phosphate (*G6P*) changes from SL to A16. *B,* schematic of muscle glucose metabolism including enzymes that increased (*red filled boxes*), decreased (*blue fill*), or were unchanged (*gray fill*) relative to CS from SL to A16 ($q < 0.05$) corresponding to data in Table S2b. *Blue bordered* enzymes decreased relative to total sample peptide from SL to A16 ($q < 0.05$). Metabolites depicted were found to increase (*red font*), decrease (*blue font*), or not change (*black font*) from SL to A16 ($q < 0.05$), or were undetected (*gray font*) by LC/MS. *C–H*, selected muscle pentose phosphate pathway intermediates (*C*), the reduced/oxidized GSH ratio (*D*), pyruvate and lactate (*E* and *F*), permeabilized muscle fiber pyruvate + malate OXPHOS capacity (*G*), and 1 carbon metabolism pathway substrates/products (*H*) at SL and A16. *3PHP*, 3-phospho-hydroxypyruvate; *DMG*, dimethylglycine; *PGL*, phosphoglucolactone; *SH7P*, sedohepulose-7-phosphate; *GAP*, glyceraldehyde-3-phosphate. *, $q <$ 0.05 *versus* SL in FDR-adjusted paired *t* tests.

chondrial NADH oxidation, which is vital for sustaining muscle energetics and cytosolic redox potential (42, 43). Consistent with this interpretation, muscle levels of malate and aspartate both increased at A16, whereas the NAD+/NADH ratio remained stable (Fig. 2*E*). Therefore, elevated PNC/MAS flux under resting conditions may be a key adaptive response to maintain muscle redox homeostasis and increase the cytosolic ATP/ADP ratio. This may in turn exert allosteric control over metabolic substrate utilization and bioenergetic flux in hypoxia.

Hypoxia directs muscle glucose utilization toward biosynthetic pathways

Consistent with a greater reliance on glucose metabolism in hypoxia reported in most studies (7), higher serum and muscle lactate, lower serum glucose, and higher muscle glucose and glucose 6-phosphate (Glc-6-P) reflect greater muscle utilization of both circulating and intramuscular glucose stores at A16 (Fig. 3*A*). This is complimented by higher CS-normalized levels of muscle hexokinase and glycogen metabolism enzymes, but not subsequent enzymes catalyzing the "investment phase" of the glycolytic pathway (Fig. 3*B*). As discussed above, the higher cytosolic ATP/ADP ratio at A16 favors inhibition of glycolysis at phosphofructokinase (PFK), which diverts Glc-6-P toward glycogen synthesis and the pentose phosphate pathway (PPP) under conditions of increased glucose availability. Parallel elevations in 6-phosphogluconolactone (PGL) and sedoheptulose 7-phosphate (SH7P), intermediates of the oxidative and non-oxidative phases of the PPP, suggest that flux through this pathway is indeed elevated at A16 (Fig. 3*C*). The PPP generates ribose sugars for nucleotide synthesis and is a primary source of cellular NADPH, which maintains a favorable reduced/oxidized GSH ratio (GSH/GSSG, Fig. 3*D*) required for cytosolic antioxidant defense by the GSH peroxidase system. Therefore, diverting glucose to the PPP may help mitigate effects of muscle adenosine degradation in hypoxia by supporting nucleotide salvage and neutralizing H_2O_2 generated by xanthine oxidase, as is increasingly appreciated in cancer cell metabolism (44).

The PPP ultimately generates glyceraldehyde 3-phosphate (GAP), which also increased at A16 (Fig. 3*E*) and can re-enter the distal portion of the glycolytic pathway at glyceraldehyde-3-phosphate dehydrogenase (GAPDH). This reaction requires NAD^+ as a cofactor, which must be regenerated from NADH oxidation in the cytosol. This can be accomplished by MAS activity or cytosolic glycerol-3-phosphate dehydrogenase (G3PDHc), both of which rely on mitochondrial reactions to maintain cytosolic NAD^+. G3PDHc increased relative to CS at A16, as well as the mitochondrial NADH:NADPH transhydrogenase and catalytic subunits of CI (Fig. 3*B*), consistent with mitochondrial adaptations that favor preservation of cytosolic redox potential in hypoxia.

Lactate dehydrogenase also supports cytosolic NADH oxidation, but was not significantly elevated at A16, despite higher muscle and serum lactate levels. Interestingly, pyruvate levels uniformly declined from SL to A16 in all but one individual, in contrast to the variable increases seen in lactate and upstream glycolytic intermediates (Fig. 3*F*). Pyruvate OXPHOS capacity was maintained in muscle fibers at A16 (Fig. 3*G*), but was likely inhibited at pyruvate dehydrogenase by higher ATP/ADP under resting conditions *in vivo*. Higher ATP and alanine observed at A16 also favor allosteric inhibition of pyruvate kinase (PK), suggesting a potential block in pyruvate formation from upstream glycolytic intermediates. However, glycolytic enzymes immediately upstream of PK increased relative to CS, particularly phosphoglycerate kinase (PGK), which is the only glycolytic enzyme that significantly increased relative to total peptide at A16 (Fig. 3*B* center, Table S2b). In addition to fueling glycolytic enzymes downstream, the product of PGK can be oxidized to 3-phospho-hydroxypyruvate. This reaction links glycolysis to one-carbon metabolism (1CM) pathways (45), which comprise the folate and methionine cycles and trans-sulfuration reactions to generate an array of products including purines, creatine, and GSH (Fig. S2) (46). Muscle 3-phospho-hydroxypyruvate levels increased uniformly in all participants from SL to A16, along with multiple 1CM pathway metabolites

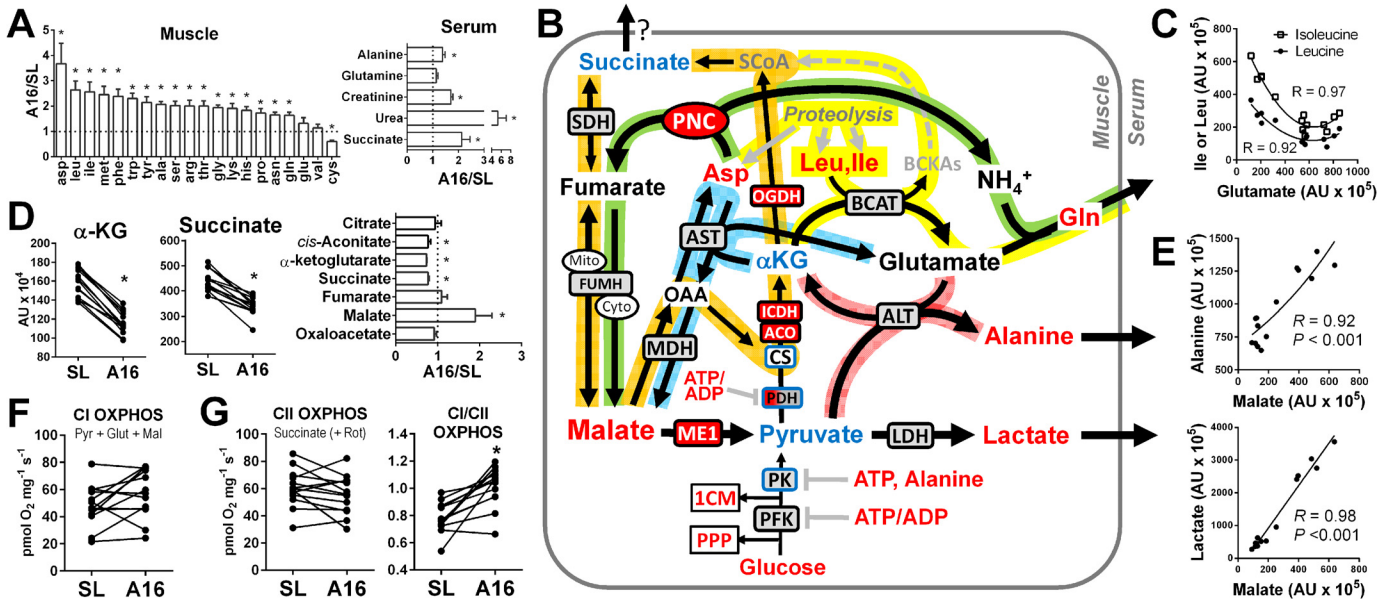

Figure 4. Muscle proteolysis alters balance of CAC intermediates in hypoxia. *A,* accumulated muscle-free amino acids and serum metabolites reflecting increased muscle proteolysis at A16. *B,* schematic summary of principal muscle amino acid catabolism reactions (*yellow path*) and their interaction with the canonical CAC (*orange path*), malate-aspartate shuttle (*blue path*), PNC (*green path*), and pyruvate transamination (*pink path*). Enzymes shown in *boxes* were found to increase (*red fill*), decrease (*blue fill*), or not change (*gray fill*) from SL to A16 relative to CS in the muscle proteome corresponding to data in Table S2b ($q < 0.05$). Metabolites depicted increased (*red font*), decreased (*blue font*), or did not change (*black font*) from SL to A16 ($q < 0.05$), or were undetected (*gray font*) by LC/MS. *C,* correlations (second order polynomial) of muscle leucine (Leu) and isoleucine (Ile) with glutamate. *D,* selective loss of muscle CAC intermediates between citrate and fumarate from SL to A16. *E,* correlations of muscle malate with alanine (exponential) and lactate (linear). ADP-stimulated (OXPHOS) respiration of permeabilized muscle fibers with substrates linked to CI (pyruvate + glutamate + malate) (*F*), CII (succinate + rotenone), and the ratio of the two (CI/CII) (G) ($n = 12–14$). *PPP*, pentose phosphate pathway; *1CM*, one-carbon metabolism; *, $q < 0.05$ A16 *versus* SL.

including dimethylglycine and taurine (Fig. 3*H*). Canonical functions of 1CM include nucleotide biosynthesis, amino acid homeostasis, and epigenetic regulation (by methylation) in the context of development and cell proliferation (46). Accordingly, there is increasing focus on the role of 1CM in cancer metabolism and growth (47), which has revealed additional functions including mitochondrial NADPH production and redox control in hypoxia (48). To our knowledge, this is the first evidence linking 1CM to hypoxia adaptation in skeletal muscle, where it might balance increases in purine nucleotide degradation and support cytosolic redox balance in conjunction with PPP activity.

Taken together, these analyses indicate that 16 days of physiological hypoxia directs increases in muscle glucose toward biosynthetic PPP and 1CM pathways, which may be critical for maintaining myocyte homeostasis. A greater reliance on glucose metabolism in hypoxia is often attributed to an up-regulation of glycolytic enzymes by HIF-1α to enhance anaerobic ATP production (5, 16). Consistent with this mechanism, we observed subtle increases in HIF-dependent HK, PGK, and AMP deaminase at A16, which catalyze key reactions in the scheme presented above. However, other HIF-regulated enzymes, most notably PFK and PK, were unchanged or lower at A16, indicating a more complex fine-tuning of glucose metabolism. Expression of PPP and 1CM enzymes was generally unaffected by hypoxia, but shunts to these pathways could occur independently through inhibition of PFK and PK by observed elevations in ATP and alanine under resting conditions (Fig. 3*B*). We propose that this allosteric regulation of basal glucose metabolism is a central feature of physiological hypoxia adaptation in skeletal muscle, driven in part by elevations in PNC and MAS activity in response to an accumulation of amino acids from protein catabolism. This hypothesis was further explored by integrating our datasets in the context of amino acid metabolism in the following section.

Muscle proteolysis supports PNC/MAS flux and anaplerotic imbalance in hypoxia

Muscle proteolysis is a well-established phenomenon in hypoxia (49, 50), and occurred in the present study as evidenced by the accumulation of 17 proteinogenic amino acids in muscle, and elevated serum levels of alanine, creatinine, and urea at A16 (Fig. 4*A*). Protein catabolism may be protective in hypoxia for several reasons (27), but also requires myocytes to balance accumulating anaplerotic carbons and amino nitrogen with cataplerotic reactions to rid the cell of ammonia while meeting cellular energy demands (51). The majority of amino nitrogen is released from skeletal muscle as alanine and glutamine, which are synthesized from other amino acids using pyruvate and α-ketoglutarate (α-KG) as carbon backbones. The branched-chain amino acids (BCAAs) leucine (Leu) and isoleucine (Ile) are primary mediators of alanine and glutamine biosynthesis (52), and along with aspartate (Asp), were the most robustly elevated free amino acids in muscle at A16 (Fig. 4*A*). Therefore, we evaluated the potential metabolic fates of these amino acids and their metabolites in the context of established protein catabolism and anaplerotic pathways (Fig. 4*B*).

BCAA catabolism in skeletal muscle begins with the transamination of α-KG to glutamate by branched-chain aminotransferase, yielding branched-chain ketoacids that are ultimately oxidized as succinyl-CoA in the citric acid cycle (CAC) (Fig. 4*B*, *yellow path*). Elevated Asp and PNC flux at A16 favor

conversion of glutamate to glutamine (Gln), which is released from muscle as a means of ridding the cell of ammonia (53) (Fig. 4*B*, *green path*). Although serum Gln was not elevated at A16 (Fig. 4*A*), it is preferentially uptaken and oxidized by kidney under conditions of metabolic acidosis to maintain acid-base balance (54). We found robust inverse correlations between muscle glutamate and both Leu and Ile levels at A16 (Fig. 4*C*) consistent with enhanced BCAA catabolism through this pathway (52). However, glutamate can also serve as the substrate for transamination of pyruvate by alanine transaminase (ALT), which regenerates αKG and promotes muscle nitrogen release as alanine (Fig. 4*B*, *red path*). Higher muscle Asp at A16 also supports this reaction by maintaining a favorable glutamate/α-KG ratio catalyzed by aspartate aminotransferase (Fig. 4*B*, *blue path*). Importantly, all these pathways favor an accumulation of malate and net loss of α-KG, generating an anaplerotic imbalance upstream of fumarate that was observed at A16 (Fig. 4*D*). Under these conditions, the majority of malate is likely generated in the cytosol by PNC/MAS activity, where it can be decarboxylated to pyruvate by cytosolic malic enzyme (ME1). ME1 strongly favors pyruvate production in human skeletal muscle (55), and increased relative to CS at A16 in the present study (Fig. 4*B*, Table S2*b*). Therefore, we hypothesize that higher malate flux through ME1 plays a key role in coupling the alanine transaminase and aspartate aminotransferase reactions to support feed-forward muscle nitrogen release from protein and nucleotide catabolism in hypoxia. Strong positive correlations of malate with alanine and lactate at A16 support this hypothesis (Fig. 4*E*), and suggest that ME1 could be a major source of pyruvate in hypoxia when ATP demand is low. This would help to preserve upstream glycolytic intermediates for the PPP and 1CM, and limit loss of α-KG needed to maintain basal levels of oxidative metabolism in hypoxia.

The pathways illustrated in Fig. 4*B* rely on mitochondrial NADH oxidation to support dehydrogenase reactions in BCAA catabolism and the MAS, which is accomplished primarily by the NADH dehydrogenase in CI of the mitochondrial respiratory system. We evaluated CI-dependent OXPHOS capacity of muscle fibers with a combination of malate, pyruvate, and glutamate as substrates, and found no change from SL to A16 (Fig. 4*F*). This parallels the observed preservation of pyruvate OXPHOS capacity (Fig. 3*E*), and indicates that the selective loss of CAC intermediates upstream of fumarate at A16 is not due to reduced muscle oxidative capacity. In fact, the three CAC enzymes downstream of citrate were increased relative to CS at A16 (Fig. 4*B*, Table S2*b*), consistent with a relative increase in the capacity to generate and oxidize α-KG in hypoxia. Succinate OXPHOS capacity (supported by succinate dehydrogenase, or mitochondrial Complex II, CII) was unchanged from SL to A16, but declined relative to the CI-linked OXPHOS capacity (Fig. 4*G*). This is consistent with the greater reliance on NADH oxidation and a re-routing of CAC intermediates that favors either reduced synthesis of succinate, or perhaps its extrusion from the cell along with lactate and alanine (56). Release of succinate from muscle or other tissues would explain its observed accumulation in serum at A16 (Fig. 4*A*), where it can promote adaptive responses through its role as a pleiotropic endocrine/paracrine signaling molecule (57). However, the resulting anaplerotic imbalance might impair muscle mitochondrial capacity to meet the elevated energy demands *in vivo* (*e.g.* during exercise) (52), compounding the limitations of reduced O_2 delivery and perhaps favoring the loss of muscle mitochondrial capacity reported following more prolonged or energetically taxing hypoxic exposures (*e.g.* trekking and climbing expeditions) (8).

Taken together, these analyses suggest that protein catabolism plays a central role in muscle metabolic responses to hypoxia by promoting a loss of α-KG and accumulation of malate. This supports adaptive shifts in glucose utilization that balance increases in catabolic stress, while contributing to basal energy production and redox homeostasis through mitochondrial NADH oxidation. In addition, α-KG is a rate-limiting cofactor for HIF-1α hydroxylation by prolyl hydroxylase domain proteins (58), which mediate proteasomal degradation of HIF-1α under basal conditions (59). Thus, α-KG cataplerosis due to protein and nucleotide catabolism at A16 could favor HIF-1α stabilization independent of changes in muscle PO_2, further promoting adaptive responses in hypoxia. However, limiting the depletion of α-KG is critical for maintaining metabolic homeostasis under these conditions. This requires sustained anaplerotic input from sources other than pyruvate and glutamate, which tend to be inhibited or depleted as discussed above. Therefore, we next evaluated the hypothesis that enhanced capacities for ketone or fatty acid oxidation help maintain anaplerosis to support resting skeletal muscle energy metabolism in high-altitude hypoxia.

Altered mitochondrial protein stoichiometry parallels improvements in long-chain acylcarnitine oxidation capacity

Consistent with a greater reliance on mitochondrial NADH oxidation at A16, select catalytic and accessory subunits of CI robustly increased at A16 compared with SL (Fig. 5, Table S2b). However, several other mitochondrial proteins, including two accessory CI subunits, decreased at A16. Whether these stoichiometric shifts in CI subunits represent adaptive structural modifications or transient changes in the number of intact complexes is unclear. Hypothetically, either could enhance CI interaction with other inner membrane protein complexes to support more efficient NADH oxidation and electron channeling (60, 61). Concomitant increases in CS-normalized levels of coenzyme Q6 monooxygenase (COQ6) at A16 (Fig. 5, Table S2b) suggest that ubiquinone biosynthesis may also be favored to support enhanced CI oxidation and electron transfer under conditions of abundant mixed substrate availability.

Ketones are major anaplerotic substrates when muscle proteolysis is elevated and pyruvate oxidation is limited, and so may be an important energy source for skeletal muscle in high-altitude hypoxia (27). In this study, muscle hydroxybutyrate (HB) decreased significantly from SL to A16, whereas serum HB was unchanged and isobutyrate declined (Fig. 5*A*). CS-normalized levels of hydroxyacid–oxoacid transhydrogenase increased at A16, perhaps reflecting a greater preference for muscle HB oxidation. However, this reaction could be limited by the reduced availability of α-KG discussed above, indicated by a significant loss of hydroxyglutarate that correlated closely with α-KG at A16 (Fig. 5*B*). Therefore, the capacity for muscle

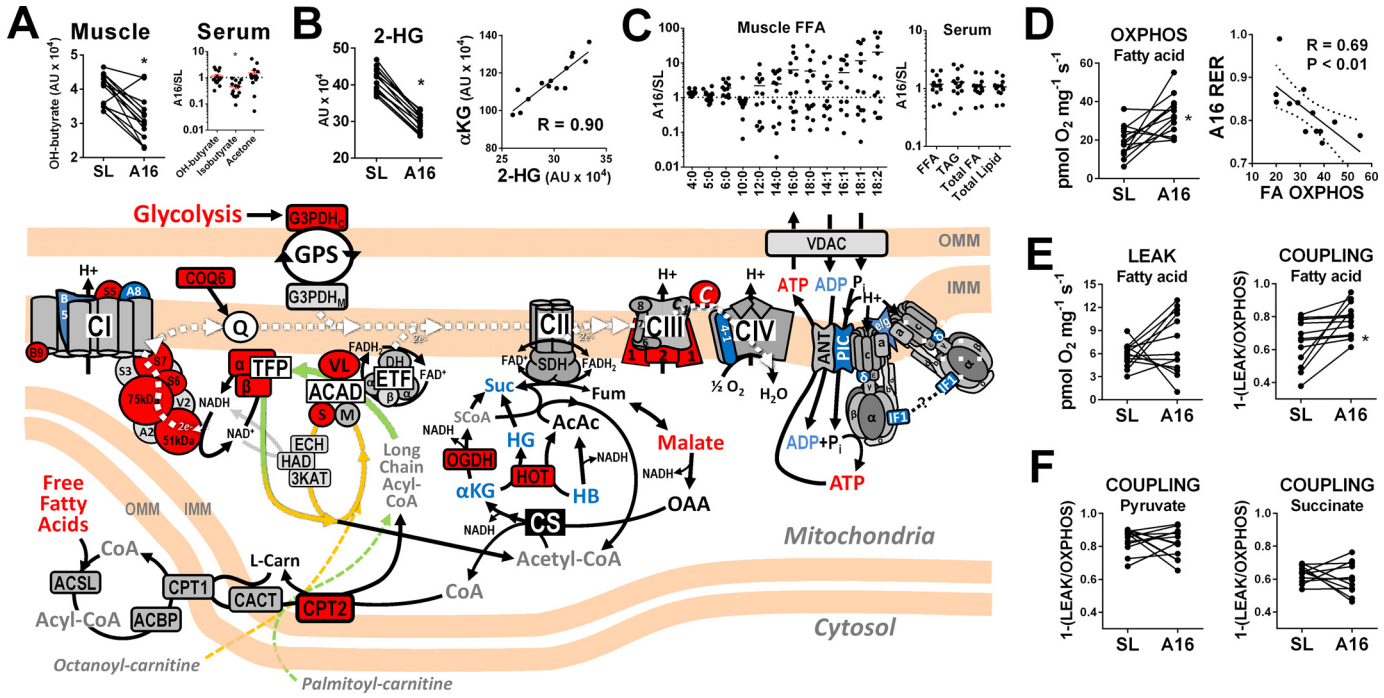

Figure 5. Ketone and fatty acid oxidation. Schematic illustrates mitochondrial fatty acid and ketone oxidation pathways with associated enzymes and electron transfer proteins that increased (*red fill*), decreased (*blue fill*), or remained unchanged (*gray fill*) relative to CS from SL to A16 (corresponding to data in Table S2b; $q < 0.05$). Metabolites shown increased (*red text*), decreased (*blue*), or did not change (*black*) from SL to A16, or were not detected by LC/MS (*gray*). *A,* muscle and serum ketones. *B,* lower muscle 2-hydroxyglutarate (*2-HG*) correlates closely with α-KG at A16. *C,* muscle fatty acids and serum lipids. *D,* higher ADP-stimulated (OXPHOS) respiratory capacity of muscle fibers with palmitoylcarnitine + malate (fatty acid) correlates inversely with systemic respiratory exchange ratio at A16 (*dotted line* represents the 95% confidence interval). *E,* no change in muscle fiber respiration in the absence of ADP (LEAK) equates to higher palmitoylcarnitine OXPHOS coupling efficiency at A16. *F,* no change in muscle pyruvate- or succinate-linked OXPHOS coupling from SL to A16. See supporting Tables S1 and S2 for complete data and abbreviation listing. *, $q < 0.05$ *versus* SL in *A* and *B*; *, $p < 0.05$ by paired *t* test in *D* and *E*.

ketone oxidation appears to be preserved or enhanced in hypoxia, but reduced substrate availability might ultimately limit its contribution to resting muscle energy metabolism.

Fatty acids are the primary energy source for resting skeletal muscle under aerobic conditions. This likely persists at A16, as evidenced by a mean RER value of 0.82 (Table 1) and similar levels of resting muscle oxygen extraction previously reported at 5260 m and SL (34). Muscle-free fatty acid levels were highly variable and tended to increase at A16, whereas serum lipids were generally unchanged (Fig. 5*C*), perhaps reflecting an increase in muscle fatty acid uptake or utilization. A greater capacity for fat oxidation in physiological hypoxia is suggested by some studies of humans (20) and animals (19) native to high-altitude environments. However, most studies of short-term hypoxia adaptation in humans have concluded either no change or a decrease, based largely on the content or activity of selected fatty acid metabolism enzymes such as β-hydroxyacyl-CoA dehydrogenase or carnitine palmitoyltransferase-1 (CPT1) (7). In agreement with these reports, muscle levels of both β-hydroxyacyl-CoA dehydrogenase and CPT1 were unchanged from SL to A16 in the present study, along with several other fatty acid transport and oxidation enzymes. However, CPT2 increased relative to CS and total peptide from SL to A16, suggesting a specific improvement in the capacity to oxidize long-chain acylcarnitines.

To investigate this hypothesis directly, we evaluated the palmitoylcarnitine-supported OXPHOS capacity of permeabilized muscle fibers at SL and A16, and found increases in nearly all participants (Fig. 5*D*). This *in vitro* measurement of muscle long-chain acylcarnitine oxidation correlated inversely with systemic RER at A16, validating its relevance to whole-body fatty acid utilization under resting conditions *in vivo*. Palmitoylcarnitine-supported respiration in the absence of ADP (LEAK) was unchanged from SL to A16, which equated to a significant improvement in palmitoylcarnitine OXPHOS coupling efficiency (Fig. 5*E*). Similar increases in OXPHOS coupling were not observed when pyruvate or succinate was used as a substrate (Fig. 5*F*), ruling out a generalized improvement in respiratory chain efficiency or phosphorylation control by the ATP synthase. This was seen despite CS-normalized decreases in cytochrome *c* oxidase subunit 4-1 (COX4-1) classically associated with HIF-1α-dependent COX subunit remodeling to improve oxygen binding in hypoxia (17). In addition, moderate decreases in multiple ATP synthase subunits and other components of the ADP phosphorylation "interactosome" (62) were observed at A16 (Fig. 5, Table S2b), despite maintenance of maximal ADP-dependent respiratory capacity in muscle fibers (Fig. S1). Whether these changes reflect an early down-regulation of mitochondrial ATP production or improvements in bioenergetic efficiency is unclear and merits further study. Collectively, these studies underscore the importance of integrated metabolic flux analysis when evaluating mitochondrial adaptations to hypoxia, and suggest that a specific enhancement of acylcarnitine oxidation capacity mediates improvements in OXPHOS coupling control observed under mixed substrate conditions (Fig. 1*C*). This might manifest *in vivo* as a greater sensitivity to ADP in low energy flux states when fatty acids serve as a primary fuel, consistent with the lower RER and

higher muscle ATP/ADP ratio observed under resting conditions at A16.

In contrast to these findings, previous studies have reported no change or a decrease in muscle acylcarnitine OXPHOS capacity following 2–4-week exposures of up to 5300 m altitude (23, 25). This discrepancy may reflect differences in the hypoxia acclimatization protocol or populations studied. However, it is also notable that these previous studies used the 8-carbon octanoylcarnitine as a substrate, which bypasses specific long-chain fatty acid oxidation enzymes on the inner mitochondrial membrane for oxidation in the canonical matrix β-oxidation cycle (Fig. 5 scheme, *orange arrow*). The 16-carbon palmitoylcarnitine used in the present study represents the long-chain fatty acids utilized by muscle *in vivo*, which require the very long-chain acyl-CoA dehydrogenase (VLCAD) for oxidation in humans (63). These are subsequently metabolized by the trifunctional protein complex (TFP; also known as long-chain acyl-CoA dehydrogenase, LCHAD), which catalyzes all three remaining reactions of the β-oxidation cycle (64) (Fig. 5 scheme, *green arrow*). Interestingly, both VLCAD and TFP increased relative to CS at A16, and localize to the inner mitochondrial membrane where they facilitate direct channeling of intermediates to the electron transferring flavoprotein and CI (65). In contrast, only a partial channeling occurs through the matrix enzymes responsible for oxidizing medium- and short-chain fatty acids (66). Inborn deficiencies in either VLCAD or TFP are associated with higher morbidity and mortality than other fatty acid oxidation enzyme defects (67, 68), underscoring their importance in fatty acid catabolism and metabolic homeostasis. We postulate that retention or up-regulation of these enzymes in hypoxia, perhaps along with CPT2 and select CI subunits, may limit toxic accumulation of acylcarnitines (69) and improve the efficiency of resting muscle energy metabolism.

Potential regulatory mechanisms

HIF-1α has been widely implicated in cellular metabolic adaptation to hypoxia (15), but its role in skeletal muscle responses to high altitude is less clear (70). We were unable to detect HIF-1α protein in any sample at SL or A16 by Western blotting in the present study, despite validating our antibody in hypoxic C2C12 myoblasts and ischemic human vastus lateralis (Fig. S3). Therefore, the significant hypoxemia observed at A16 was evidently insufficient to decrease muscle PO_2 to a level required for sustained HIF-1α stabilization under routine sedentary conditions. This is consistent with a high functional reserve of muscle oxygen diffusion capacity at high altitude (71), and suggests that muscle metabolic responses to hypoxemia (*e.g.* induction of proteolysis discussed above) likely predominate over tissue hypoxia *per se* in the present study. However, we cannot rule out the possibility that muscle HIF-1α stabilization occurred transiently during an earlier phase of hypoxia exposure, thereby partially contributing to the metabolic phenotype observed at A16.

To explore the basis for improved muscle OXPHOS capacity observed at A16, we evaluated AMP-activated protein kinase (AMPK) and GTPase optic atrophy 1 (OPA1) as established regulators of mitochondrial metabolism (72) and dynamics (73) in response to energetic stress. However, total and Thr-121

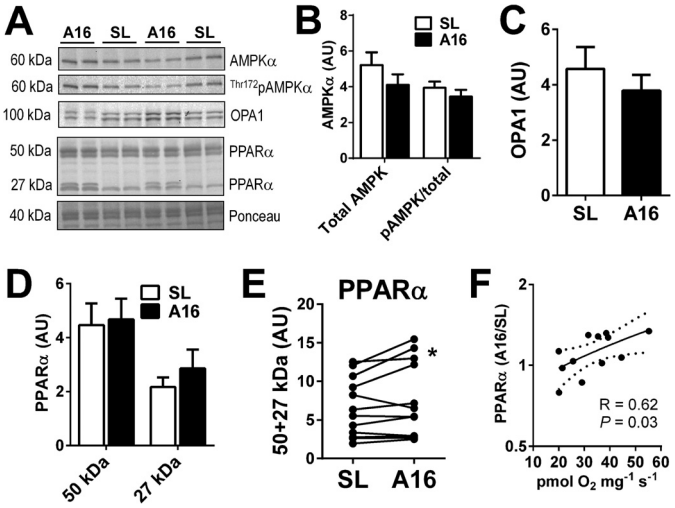

Figure 6. Putative regulators of muscle metabolic adaptation to high-altitude hypoxia. *A–D*, representative blots (*A*) and graphical summaries of muscle protein expression (20 μg) of total and phosphorylated AMP kinase-α (*AMPKα*; *B*), GTPase optic atrophy 1 (*OPA1*; *C*), and PPARα (*D*). *E*, individual subject data of paired SL and A16 (same gel) PPARα protein blots (50 + 27 kDa). *F*, paired A16/SL blot density ratios of total PPARα (50 + 27 kDa) positively correlate with palmitoylcarnitine-supported OXPHOS capacity at A16 (data from Fig. 5*E*). *, $p < 0.05$ by paired *t* test.

phosphorylated AMPK were unchanged from SL to A16 (Fig. 6*B*), consistent with the preservation of muscle AMP and higher ATP/ADP ratio (Fig. 2). OPA1 tended to decline from SL to A16 (Fig. 6*C*, $p = 0.06$), perhaps reflecting a trend toward mitochondrial cristae remodeling favoring less fusion consistent with reduced levels of prohibitins (Table S2*A*) and ATP synthase subunits (Fig. 5*A*) at A16 (74). However, it is unclear whether these changes would support the improvements in muscle OXPHOS function observed at A16.

Given the selective enhancement of fatty acid-linked OXPHOS at A16, we investigated protein levels of the peroxisome proliferator-activated receptor α (PPARα), the master transcriptional regulator of muscle fatty acid metabolism (75). We found that whereas expression at the expected molecular mass of 50 kDa was unchanged, expression of distinct bands at 27 kDa tended to increase, resulting in a higher combined protein expression at A16 in several subjects (Fig. 6*D*). The functional relevance of this 27-kDa band is unclear, but higher total PPARα expression (50 + 27 kDa band density) in paired A16/SL subject samples correlated with muscle palmitoylcarnitine OXPHOS capacity at A16 (Fig. 6, *E* and *F*), suggesting a positive regulatory role on muscle fat oxidation. Notably, PPARα haplotypes have been linked to the evolutionary adaptation of humans to high altitude (76), with unclear functional implications. Collectively, these results highlight the need for further investigation of the roles that fatty acid metabolism and PPARα play in the physiological adaptation to high altitude, and perhaps other conditions associated with chronic hypoxemia.

Summary and conclusions

Understanding the homeostatic adjustments of aerobic tissues to a low oxygen environment is essential for distinguishing adaptive from maladaptive responses in hypoxia-related conditions. Although still controversial, the prevailing view is that chronic hypoxia induces a shift from aerobic to anaerobic

metabolism that includes a down-regulation of mitochondrial capacity, favoring glycolytic over fatty acid energy supply (7). The present study demonstrates that a loss of muscle mitochondrial capacity is not obligatory for at least the early phase of high-altitude hypoxia adaptation. Rather, mitochondria play a central role in adaptive responses by supporting greater resting muscle phosphorylation potential and enhancing the efficiency of fatty acid oxidation. This favors allosteric inhibition of key regulatory enzymes in glycolysis, which directs glucose toward pentose phosphate and one-carbon metabolism pathways that support cytosolic redox balance and purine nucleotide homeostasis. Muscle accumulation of free amino acids from protein catabolism appears to be a primary driver of this response by coordinating cytosolic and mitochondrial pathways to rid the cell of ammonia. This generates an anaplerotic imbalance that may be initially adaptive, but could ultimately limit muscle oxidative capacity *in vivo* independent of oxygen availability.

These findings bear a striking resemblance to emerging perspectives on cancer metabolism, where a similarly integrated view of metabolic adaptation has begun to transcend the classic Warburg hypothesis (77). The handling of accumulated amino acids from protein catabolism may be a pivotal regulator of both systems by redirecting oxidative metabolism and facilitating either cellular remodeling or growth. Muscle wasting is a hallmark of all hypoxia-related pathologies as well as surgical trauma, advanced diabetes, aging, and cancer cachexia. Therefore, therapeutic interventions that target muscle protein catabolism might reveal unanticipated benefits in hypoxia-related conditions and certain cancers. Mechanistically, future studies are needed to define the respective contributions of the PNC, 1CM, and long-chain acylcarnitine oxidation pathways to physiological hypoxia adaptation, and the regulatory basis for associated stoichiometric shifts in the mitochondrial and cytosolic proteomes. These processes are likely to be orchestrated by a complex interplay of transcriptional, allosteric, and substrate-level regulation that will require integrative experimental approaches and interpretation to clarify further.

Experimental procedures

Human subjects and sample collection

Subjects (7 male, 7 female; 21 ± 2 years of age) were a randomly selected subset of 25 individuals studied at SL (Eugene, OR) and following 16 days at 5260 m (A16) on Mt. Chacaltaya in the Bolivian Andes during the 2012 AltitudeOmics project (26). All subjects engaged in light voluntary activity and were provided *ad libitum* meals to minimize confounding effects of negative energy balance and inactivity. All procedures conformed to the Declaration of Helsinki and were approved by the Universities of Colorado, Oregon, and Utah Institutional Review Boards and the United States Department of Defense Human Research Protection Program Office. Physiological measures in Table 1 were obtained through indirect calorimetry and pulse oximetry on the subset of subjects from the AltitudeOmics project studied in the present investigation (see supporting Materials and methods for full disclosure of data previously reported from the full subject cohort). Vastus lateralis muscle biopsies were obtained under resting post-absorptive conditions at least 24 h following any exercise using the Bergström technique under local anesthesia (1% lidocaine subcutaneously) (78). Sections (100–150 mg) were immediately placed in ice-cold biopsy preservation media (BIOPS) containing (in mM) 10 Ca^{2+}-EGTA, 20 imidazole, 50 potassium/MES, 0.5 DTT, 6.56 $MgCl_2$, 5.77 ATP, and 15 phosphocreatine at pH 7.1 for preparation of permeabilized fibers, or snap frozen in liquid nitrogen for storage at −80 °C for future biochemical analysis.

Mitochondrial respirometry

Mitochondrial metabolism was evaluated in permeabilized muscle fiber bundles prepared as previously described (29) using two Oxygraph-2k high-resolution respirometers (Oroboros Instruments, Innsbruck, Austria). Oxygen flux was monitored in real-time by resolving changes in the negative time derivative of the chamber oxygen concentration signal normalized to fiber wet weight following standardized instrumental and chemical background calibrations performed daily (instrumental) or before every experiment (chemical background). Respirometry chambers were maintained at 37 °C in a hyperoxygenated environment (275–400 μM O_2) to avoid potential limitations in oxygen diffusion on respiratory capacity of permeabilized fiber bundles (29). A detailed description of the respiration protocols and respiratory states generated by the sequential titration of each constituent are provided in Table S1. All samples were run in duplicate and averaged, and occasionally a third or fourth time if the response of repeats lacked uniformity. Any fiber preparations exhibiting a greater than 10% increase in flux in response to cytochrome *c* (indicating loss of outer mitochondrial membrane integrity) were excluded from analyses.

Metabolomic profiling

Metabolites were extracted from snap-frozen serum (10 μl) or muscle biopsies (10 mg) in ice-cold methanol/acetonitrile/water (5:3:2), separated on a Kinetex XB-C18 column (Phenomenex), and analyzed using a UHPLC system (Vanquish, Thermo, San Jose, CA) coupled to a Q Exactive quadrupole-Orbitrap mass spectrometer (Thermo, San Jose, CA). Calibration was performed before each analysis against positive or negative ion mode calibration mixes (Piercenet, Thermo Fisher, Rockford, IL) to ensure <1 ppm error of the intact mass. Metabolite selection was performed against the KEGG pathway database using Maven software (Princeton, NJ) and confirmed against a library of over 630 standard compounds (Sigma; IROATech, Bolton, MA). See supporting "Materials and methods" for a more detailed description of the metabolomic profiling procedures.

Proteomic profiling

Muscle proteomic analyses were performed by Tandem Mass Tag labeling LC-MS/MS, which enables multiplexing of sample groups to maximize the internal validity and sensitivity of treatment comparisons. Trypsin-digested samples were labeled with a unique reporter tag (TMT 10-Plex, Thermo Pierce), then subjected to offline UPLC-UV fractionation and concentration for LC-MS/MS analysis. Paired (SL and A16) samples from individual subjects were analyzed simultaneously

to determine protein abundance changes from SL to A16, using SL as the reference sample in each multiplexed pairing, with a false discovery rate (FDR) for peptides set at 0.1%. Data were searched against the human Uniprot protein database in MASCOT Server (version 2.3) and imported into Scaffold Q+S for data refinement and quantification of reporter tag intensity. A detailed description of proteomic profiling methods is provided under supporting "Materials and methods".

Western blotting

Muscle expression of selected regulatory proteins was evaluated in 20 μg of protein extracts of muscle biopsies by standard immunoblotting procedures as described previously (79). Primary antibodies were all from Cell Signaling (Danvers, MA) except PPARα (Abcam, Cambridge, MA; number 24509S) used at 1:500–1000 dilutions, normalized to actin or total protein (Ponceau S) staining for loading control.

Statistical analyses

SL and A16 data were compared by paired *t*-tests using Bonferroni-Hochberg corrections for multiple comparisons with a FDR of 0.05 for metabolomic and 0.20 for proteomic profiling to denote statistical significance at $q < 0.05$. A standard $p < 0.05$ was used for physiology and respirometry data and selected Pearson correlation analyses.

Author contributions—A. J. C., A. T. L., A. W. S., and R. C. R. conceptualization; A. J. C., E. G., H. C. D., J. E. P., A. T. L., A. W. S., and R. C. R. resources; A. J. C., C. H. L., E. G., A. D., T. N., A. D. H., J. E. P., L. M. W., N. M. S., A. T. L., and A. W. S. data curation; A. J. C., C. H. L., E. G., J. B. M., A. D., T. N., L. M. W., N. M. S., and A. W. S. formal analysis; A. J. C., J. E. P., A. T. L., A. W. S., and R. C. R. supervision; A. J. C., T. N., L. M. W., and N. M. S. validation; A. J. C., C. H. L., E. G., H. C. D., J. B. M., A. D., T. N., A. D. H., L. M. W., A. T. L., and A. W. S. investigation; A. J. C., E. G., H. C. D., A. D., T. N., J. E. P., N. M. S., and A. W. S. methodology; A. J. C. writing-original draft; A. J. C. and R. C. R. project administration; A. J. C., A. D., T. N., and R. C. R. writing-review and editing; E. G. software; A. T. L. and R. C. R. funding acquisition.

Acknowledgments—This study was part of the AltitudeOmics project that explores the basic mechanisms controlling human acclimatization to hypoxia. Many people and organizations have invested enormous amounts of time and resources to make AltitudeOmics a success. Foremost, we thank the tireless support, generosity, and tenacity of our research subjects. AltitudeOmics principal investigators were A. T. Lovering, A. W. Subudhi, and R. C. Roach. We also thank the many other investigators on this multinational, collaborative effort involved in development, subject management, and data collection, supporting industry partners, and people and organizations in Bolivia that made AltitudeOmics possible. We are extremely grateful to J. Kern, J. E. Elliot, S. S. Laurie and L. M. Beasley for their invaluable assistance in the blood gas data collection for this study.

References

1. Martin, D. S., Levett, D. Z., Grocott, M. P., and Montgomery, H. E. (2010) Variation in human performance in the hypoxic mountain environment. *Exp. Physiol.* **95,** 463–470 CrossRef Medline
2. Doehner, W., Frenneaux, M., and Anker, S. D. (2014) Metabolic impairment in heart failure: the myocardial and systemic perspective. *J. Am. Coll. Cardiol.* **64,** 1388–1400 CrossRef Medline
3. Puente-Maestu, L., Lázaro, A., and Humanes, B. (2013) Metabolic derangements in COPD muscle dysfunction. *J. Appl. Physiol.* **114,** 1282–1290 CrossRef Medline
4. Meyer, A., Zoll, J., Charles, A. L., Charloux, A., de Blay, F., Diemunsch, P., Sibilia, J., Piquard, F., and Geny, B. (2013) Skeletal muscle mitochondrial dysfunction during chronic obstructive pulmonary disease: central actor and therapeutic target. *Exp. Physiol.* **98,** 1063–1078 CrossRef Medline
5. Cerretelli, P., Marzorati, M., and Marconi, C. (2009) Muscle bioenergetics and metabolic control at altitude. *High Alt. Med. Biol.* **10,** 165–174 CrossRef Medline
6. Hoppeler, H., and Vogt, M. (2001) Muscle tissue adaptations to hypoxia. *J. Exp. Biol.* **204,** 3133–3139 Medline
7. Horscroft, J. A., and Murray, A. J. (2014) Skeletal muscle energy metabolism in environmental hypoxia: climbing towards consensus. *Extrem. Physiol. Med.* **3,** 19 CrossRef Medline
8. Murray, A. J., and Horscroft, J. A. (2016) Mitochondrial function at extreme high altitude. *J. Physiol.* **594,** 1137–1149 CrossRef Medline
9. Hochachka, P. W., Stanley, C., Merkt, J., and Sumar-Kalinowski, J. (1983) Metabolic meaning of elevated levels of oxidative enzymes in high altitude adapted animals: an interpretive hypothesis. *Respir. Physiol.* **52,** 303–313 CrossRef Medline
10. Kayser, B., Hoppeler, H., Desplanches, D., Marconi, C., Broers, B., and Cerretelli, P. (1996) Muscle ultrastructure and biochemistry of lowland Tibetans. *J. Appl. Physiol.* **81,** 419–425 CrossRef Medline
11. Kayser, B., Hoppeler, H., Claassen, H., and Cerretelli, P. (1991) Muscle structure and performance capacity of Himalayan Sherpas. *J. Appl. Physiol.* **70,** 1938–1942 CrossRef Medline
12. Levett, D. Z., Radford, E. J., Menassa, D. A., Graber, E. F., Morash, A. J., Hoppeler, H., Clarke, K., Martin, D. S., Ferguson-Smith, A. C., Montgomery, H. E., Grocott, M. P., Murray, A. J., and Caudwell Xtreme Everest Research, G. (2012) Acclimatization of skeletal muscle mitochondria to high-altitude hypoxia during an ascent of Everest. *FASEB J.* **26,** 1431–1441 CrossRef
13. Edwards, L. M., Murray, A. J., Tyler, D. J., Kemp, G. J., Holloway, C. J., Robbins, P. A., Neubauer, S., Levett, D., Montgomery, H. E., Grocott, M. P., Clarke, K., and Caudwell Xtreme Everest Research Group (2010) The effect of high-altitude on human skeletal muscle energetics: P-MRS results from the Caudwell Xtreme Everest expedition. *PloS One* **5,** e10681 CrossRef Medline
14. Green, H. J., Sutton, J. R., Wolfel, E. E., Reeves, J. T., Butterfield, G. E., and Brooks, G. A. (1992) Altitude acclimatization and energy metabolic adaptations in skeletal muscle during exercise. *J. Appl. Physiol.* **73,** 2701–2708 CrossRef Medline
15. Kim, J. W., Tchernyshyov, I., Semenza, G. L., and Dang, C. V. (2006) HIF-1-mediated expression of pyruvate dehydrogenase kinase: a metabolic switch required for cellular adaptation to hypoxia. *Cell Metab.* **3,** 177–185 CrossRef Medline
16. Semenza, G. L., Roth, P. H., Fang, H. M., and Wang, G. L. (1994) Transcriptional regulation of genes encoding glycolytic enzymes by hypoxia-inducible factor 1. *J. Biol. Chem.* **269,** 23757–23763 Medline
17. Fukuda, R., Zhang, H., Kim, J. W., Shimoda, L., Dang, C. V., and Semenza, G. L. (2007) HIF-1 regulates cytochrome oxidase subunits to optimize efficiency of respiration in hypoxic cells. *Cell* **129,** 111–122 CrossRef Medline
18. Roberts, A. C., Butterfield, G. E., Cymerman, A., Reeves, J. T., Wolfel, E. E., and Brooks, G. A. (1996) Acclimatization to 4,300-m altitude decreases reliance on fat as a substrate. *J. Appl. Physiol.* **81,** 1762–1771 CrossRef Medline
19. Cheviron, Z. A., Bachman, G. C., Connaty, A. D., McClelland, G. B., and Storz, J. F. (2012) Regulatory changes contribute to the adaptive enhancement of thermogenic capacity in high-altitude deer mice. *Proc. Natl. Acad. Sci. U.S.A.* **109,** 8635–8640 CrossRef Medline
20. Gelfi, C., De Palma, S., Ripamonti, M., Eberini, I., Wait, R., Bajracharya, A., Marconi, C., Schneider, A., Hoppeler, H., and Cerretelli, P. (2004) New aspects of altitude adaptation in Tibetans: a proteomic approach. *FASEB J.* **18,** 612–614 CrossRef
21. Young, A. J., Evans, W. J., Cymerman, A., Pandolf, K. B., Knapik, J. J., and Maher, J. T. (1982) Sparing effect of chronic high-altitude exposure on

muscle glycogen utilization. *J. Appl. Physiol.* **52,** 857–862 CrossRef Medline
22. Jacobs, R. A., Lundby, A. K., Fenk, S., Gehrig, S., Siebenmann, C., Flück, D., Kirk, N., Hilty, M. P., and Lundby, C. (2016) Twenty-eight days of exposure to 3454 m increases mitochondrial volume density in human skeletal muscle. *J. Physiol.* **594,** 1151–1166 CrossRef Medline
23. Jacobs, R. A., Siebenmann, C., Hug, M., Toigo, M., Meinild, A. K., and Lundby, C. (2012) Twenty-eight days at 3454-m altitude diminishes respiratory capacity but enhances efficiency in human skeletal muscle mitochondria. *FASEB J.* **26,** 5192–5200 CrossRef
24. Levett, D. Z., Viganó, A., Capitanio, D., Vasso, M., De Palma, S., Moriggi, M., Martin, D. S., Murray, A. J., Cerretelli, P., Grocott, M. P., and Gelfi, C. (2015) Changes in muscle proteomics in the course of the Caudwell Research Expedition to Mt. Everest. *Proteomics* **15,** 160–171 CrossRef Medline
25. Horscroft, J. A., Kotwica, A. O., Laner, V., West, J. A., Hennis, P. J., Levett, D. Z., Howard, D. J., Fernandez, B. O., Burgess, S. L., Ament, Z., Gilbert-Kawai, E. T., Vercueil, A., Landis, B. D., Mitchell, K., Mythen, M. G., *et al.* (2017) Metabolic basis to Sherpa altitude adaptation. *Proc. Natl. Acad. Sci. U.S.A.* **114,** 6382–6387 CrossRef Medline
26. Subudhi, A. W., Bourdillon, N., Bucher, J., Davis, C., Elliott, J. E., Eutermoster, M., Evero, O., Fan, J. L., Jameson-Van Houten, S., Julian, C. G., Kark, J., Kark, S., Kayser, B., Kern, J. P., Kim, S. E., *et al.* (2014) AltitudeOmics: the integrative physiology of human acclimatization to hypobaric hypoxia and its retention upon reascent. *PLoS ONE* **9,** e92191 CrossRef Medline
27. Murray, A. J., and Montgomery, H. E. (2014) How wasting is saving: weight loss at altitude might result from an evolutionary adaptation. *BioEssays* **36,** 721–729 CrossRef
28. Bender, P. R., McCullough, R. E., McCullough, R. G., Huang, S. Y., Wagner, P. D., Cymerman, A., Hamilton, A. J., and Reeves, J. T. (1989) Increased exercise SaO_2 independent of ventilatory acclimatization at 4,300 m. *J. Appl. Physiol.* **66,** 2733–2738 CrossRef Medline
29. Pesta, D., and Gnaiger, E. (2012) High-resolution respirometry: OXPHOS protocols for human cells and permeabilized fibers from small biopsies of human muscle. *Methods Mol. Biol.* **810,** 25–58 CrossRef Medline
30. van den Borst, B., Slot, I. G., Hellwig, V. A., Vosse, B. A., Kelders, M. C., Barreiro, E., Schols, A. M., and Gosker, H. R. (2013) Loss of quadriceps muscle oxidative phenotype and decreased endurance in patients with mild-to-moderate COPD. *J. Appl. Physiol.* **114,** 1319–1328 CrossRef Medline
31. Gosker, H. R., Wouters, E. F., van der Vusse, G. J., and Schols, A. M. (2000) Skeletal muscle dysfunction in chronic obstructive pulmonary disease and chronic heart failure: underlying mechanisms and therapy perspectives. *Am. J. Clin. Nutr.* **71,** 1033–1047 CrossRef Medline
32. Larsen, S., Nielsen, J., Hansen, C. N., Nielsen, L. B., Wibrand, F., Stride, N., Schroder, H. D., Boushel, R., Helge, J. W., Dela, F., and Hey-Mogensen, M. (2012) Biomarkers of mitochondrial content in skeletal muscle of healthy young human subjects. *J. Physiol.* **590,** 3349–3360 CrossRef Medline
33. Schlattner, U., Tokarska-Schlattner, M., and Wallimann, T. (2006) Mitochondrial creatine kinase in human health and disease. *Biochim. Biophys. Acta* **1762,** 164–180 CrossRef Medline
34. Calbet, J. A., Boushel, R., Radegran, G., Sondergaard, H., Wagner, P. D., and Saltin, B. (2003) Why is VO_2max after altitude acclimatization still reduced despite normalization of arterial O2 content? *Am. J. Physiol. Regul. Integr. Comp. Physiol.* **284,** R304–R316 CrossRef
35. Pouw, E. M., Schols, A. M., van der Vusse, G. J., and Wouters, E. F. (1998) Elevated inosine monophosphate levels in resting muscle of patients with stable chronic obstructive pulmonary disease. *Am. J. Respir. Crit. Care Med.* **157,** 453–457 CrossRef Medline
36. Delample, D., Durand, F., Severac, A., Belghith, M., Mas, E., Michel, F., Cristol, J. P., Hayot, M., and Prefaut, C. (2008) Implication of xanthine oxidase in muscle oxidative stress in COPD patients. *Free Radic. Res.* **42,** 807–814 CrossRef Medline
37. Korzeniewski, B. (2006) AMP deamination delays muscle acidification during heavy exercise and hypoxia. *J. Biol. Chem.* **281,** 3057–3066 CrossRef Medline
38. Sahlin, K., and Broberg, S. (1990) Adenine nucleotide depletion in human muscle during exercise: causality and significance of AMP deamination. *Int. J. Sports Med.* **11,** S62–S67 CrossRef Medline
39. Wu, J., Bond, C., Chen, P., Chen, M., Li, Y., Shohet, R. V., and Wright, G. (2015) HIF-1α in the heart: remodeling nucleotide metabolism. *J. Mol. Cell. Cardiol.* **82,** 194–200 CrossRef Medline
40. Liu, Y. C., Li, F., Handler, J., Huang, C. R., Xiang, Y., Neretti, N., Sedivy, J. M., Zeller, K. I., and Dang, C. V. (2008) Global regulation of nucleotide biosynthetic genes by c-Myc. *PloS One* **3,** e2722 CrossRef Medline
41. Gordan, J. D., Thompson, C. B., and Simon, M. C. (2007) HIF and c-Myc: sibling rivals for control of cancer cell metabolism and proliferation. *Cancer Cell* **12,** 108–113 CrossRef Medline
42. Arinze, I. J. (2005) Facilitating understanding of the purine nucleotide cycle and the one-carbon pool: Part I: the purine nucleotide cycle. *Biochem. Mol. Biol. Ed.* **33,** 165–168 CrossRef
43. Goodman, M. N., and Lowenstein, J. M. (1977) The purine nucleotide cycle. Studies of ammonia production by skeletal muscle *in situ* and in perfused preparations. *J. Biol. Chem.* **252,** 5054–5060 Medline
44. Patra, K. C., and Hay, N. (2014) The pentose phosphate pathway and cancer. *Trends Biochem. Sci.* **39,** 347–354 CrossRef Medline
45. Fell, D. A., and Snell, K. (1988) Control analysis of mammalian serine biosynthesis: feedback inhibition on the final step. *Biochem. J.* **256,** 97–101 CrossRef Medline
46. Ducker, G. S., and Rabinowitz, J. D. (2017) One-carbon metabolism in health and disease. *Cell Metab.* **25,** 27–42 Medline
47. Locasale, J. W. (2013) Serine, glycine and one-carbon units: cancer metabolism in full circle. *Nat. Rev. Cancer* **13,** 572–583 CrossRef Medline
48. Ye, J., Fan, J., Venneti, S., Wan, Y. W., Pawel, B. R., Zhang, J., Finley, L. W., Lu, C., Lindsten, T., Cross, J. R., Qing, G., Liu, Z., Simon, M. C., Rabinowitz, J. D., and Thompson, C. B. (2014) Serine catabolism regulates mitochondrial redox control during hypoxia. *Cancer Dis.* **4,** 1406–1417 CrossRef Medline
49. Boyer, S. J., and Blume, F. D. (1984) Weight loss and changes in body composition at high altitude. *J. Appl. Physiol.* **57,** 1580–1585 CrossRef Medline
50. Chaudhary, P., Suryakumar, G., Prasad, R., Singh, S. N., Ali, S., and Ilavazhagan, G. (2012) Chronic hypobaric hypoxia mediated skeletal muscle atrophy: role of ubiquitin-proteasome pathway and calpains. *Mol. Cell. Biochem.* **364,** 101–113 CrossRef Medline
51. Owen, O. E., Kalhan, S. C., and Hanson, R. W. (2002) The key role of anaplerosis and cataplerosis for citric acid cycle function. *J. Biol. Chem.* **277,** 30409–30412 CrossRef Medline
52. Wagenmakers, A. J. (1998) Protein and amino acid metabolism in human muscle. *Adv. Exp. Med. Biol.* **441,** 307–319 CrossRef Medline
53. Graham, T. E., and MacLean, D. A. (1998) Ammonia and amino acid metabolism in skeletal muscle: human, rodent and canine models. *Med. Sci. Sports Exerc.* **30,** 34–46 Medline
54. Welbourne, T. C. (1987) Interorgan glutamine flow in metabolic acidosis. *Am. J. Physiol.* **253,** F1069–F1076 Medline
55. Taroni, F., and Di Donato, S. (1988) Purification and properties of cytosolic malic enzyme from human skeletal muscle. *Int. J. Biochem.* **20,** 857–866 CrossRef Medline
56. Taegtmeyer, H. (1978) Metabolic responses to cardiac hypoxia. Increased production of succinate by rabbit papillary muscles. *Circ. Res.* **43,** 808–815 CrossRef Medline
57. Tretter, L., Patocs, A., and Chinopoulos, C. (2016) Succinate, an intermediate in metabolism, signal transduction, ROS, hypoxia, and tumorigenesis. *Biochim. Biophys. Acta* **1857,** 1086–1101 CrossRef Medline
58. Markolovic, S., Wilkins, S. E., and Schofield, C. J. (2015) Protein hydroxylation catalyzed by 2-oxoglutarate-dependent oxygenases. *J. Biol. Chem.* **290,** 20712–20722 CrossRef Medline
59. Semenza, G. L. (2007) Hypoxia-inducible factor 1 (HIF-1) pathway. *Science's STKE* 2007, cm8 Medline
60. Wu, M., Gu, J., Guo, R., Huang, Y., and Yang, M. (2016) Structure of mammalian respiratory supercomplex I1III2IV1. *Cell* **167,** 1598–1609.e10 CrossRef Medline
61. Zhu, J., Vinothkumar, K. R., and Hirst, J. (2016) Structure of mammalian respiratory complex I. *Nature* **536,** 354–358 CrossRef Medline

62. Chen, C., Ko, Y., Delannoy, M., Ludtke, S. J., Chiu, W., and Pedersen, P. L. (2004) Mitochondrial ATP synthasome: three-dimensional structure by electron microscopy of the ATP synthase in complex formation with carriers for P_i and ADP/ATP. *J. Biol. Chem.* **279,** 31761–31768 CrossRef Medline
63. Maher, A. C., Mohsen, A. W., Vockley, J., and Tarnopolsky, M. A. (2010) Low expression of long-chain acyl-CoA dehydrogenase in human skeletal muscle. *Mol. Genet. Metab.* **100,** 163–167 CrossRef Medline
64. Eaton, S., Bursby, T., Middleton, B., Pourfarzam, M., Mills, K., Johnson, A. W., and Bartlett, K. (2000) The mitochondrial trifunctional protein: centre of a β-oxidation metabolon? *Biochem. Soc. Trans.* **28,** 177–182 CrossRef Medline
65. Wang, Y., Mohsen, A. W., Mihalik, S. J., Goetzman, E. S., and Vockley, J. (2010) Evidence for physical association of mitochondrial fatty acid oxidation and oxidative phosphorylation complexes. *J. Biol. Chem.* **285,** 29834–29841 CrossRef Medline
66. Nada, M. A., Rhead, W. J., Sprecher, H., Schulz, H., and Roe, C. R. (1995) Evidence for intermediate channeling in mitochondrial β-oxidation. *J. Biol. Chem.* **270,** 530–535 CrossRef Medline
67. Aoyama, T., Souri, M., Ushikubo, S., Kamijo, T., Yamaguchi, S., Kelley, R. I., Rhead, W. J., Uetake, K., Tanaka, K., and Hashimoto, T. (1995) Purification of human very-long-chain acyl-coenzyme A dehydrogenase and characterization of its deficiency in seven patients. *J. Clin. Invest.* **95,** 2465–2473 CrossRef Medline
68. Spiekerkoetter, U. (2010) Mitochondrial fatty acid oxidation disorders: clinical presentation of long-chain fatty acid oxidation defects before and after newborn screening. *J. Inherited Metab. Dis.* **33,** 527–532 CrossRef Medline
69. McCoin, C. S., Knotts, T. A., and Adams, S. H. (2015) Acylcarnitines: old actors auditioning for new roles in metabolic physiology. *Nat. Rev. Endocrinol.* **11,** 617–625 CrossRef Medline
70. Lundby, C., Pilegaard, H., Andersen, J. L., van Hall, G., Sander, M., and Calbet, J. A. (2004) Acclimatization to 4100 m does not change capillary density or mRNA expression of potential angiogenesis regulatory factors in human skeletal muscle. *J. Exp. Biol.* **207,** 3865–3871 CrossRef Medline
71. Calbet, J. A., and Lundby, C. (2009) Air to muscle O2 delivery during exercise at altitude. *High Alt. Med. Biol.* **10,** 123–134 CrossRef Medline
72. Marin, T. L., Gongol, B., Zhang, F., Martin, M., Johnson, D. A., Xiao, H., Wang, Y., Subramaniam, S., Chien, S., and Shyy, J. Y. AMPK promotes mitochondrial biogenesis and function by phosphorylating the epigenetic factors DNMT1, RBBP7, and HAT1. *Sci. Signal.* **10**
73. Mishra, P., and Chan, D. C. (2016) Metabolic regulation of mitochondrial dynamics. *J. Cell Biol.* **212,** 379–387 Medline
74. Merkwirth, C., Martinelli, P., Korwitz, A., Morbin, M., Brönneke, H. S., Jordan, S. D., Rugarli, E. I., and Langer, T. (2012) Loss of prohibitin membrane scaffolds impairs mitochondrial architecture and leads to tau hyperphosphorylation and neurodegeneration. *PLoS Genet.* **8,** e1003021 CrossRef Medline
75. Kersten, S. (2014) Integrated physiology and systems biology of PPARα. *Mol. Metab.* **3,** 354–371 Medline
76. Simonson, T. S., Yang, Y., Huff, C. D., Yun, H., Qin, G., Witherspoon, D. J., Bai, Z., Lorenzo, F. R., Xing, J., Jorde, L. B., Prchal, J. T., and Ge, R. (2010) Genetic evidence for high-altitude adaptation in Tibet. *Science* **329,** 72–75 Medline
77. DeBerardinis, R. J., and Chandel, N. S. (2016) Fundamentals of cancer metabolism. *Sci. Adv.* **2,** e1600200 CrossRef Medline
78. Dreyer, H. C., Fujita, S., Cadenas, J. G., Chinkes, D. L., Volpi, E., and Rasmussen, B. B. (2006) Resistance exercise increases AMPK activity and reduces 4E-BP1 phosphorylation and protein synthesis in human skeletal muscle. *J. Physiol* **576,** 613–624 CrossRef Medline
79. Hocker, A. D., Boileau, R. M., Lantz, B. A., Jewett, B. A., Gilbert, J. S., and Dreyer, H. C. (2013) Endoplasmic reticulum stress activation during total knee arthroplasty. *Physiol. Rep.* **1,** e00052 Medline